Applied Surface Science 371 (2016) 139–150

Contents lists available at ScienceDirect

Applied Surface Science

journal homepage: www.elsevier.com/locate/apsusc

Adhesion and inactivation of Gram-negative and Gram-positive bacteria on photoreactive TiO_2/polymer and Ag–TiO_2/polymer nanohybrid films

Szabolcs Péter Tallósy[a,b], László Janovák[b], Elisabeth Nagy[a], Ágota Deák[b], Ádám Juhász[c], Edit Csapó[c], Norbert Buzás[d], Imre Dékány[c,*]

[a] Institute of Clinical Microbiology, Faculty of Medicine, University of Szeged, H-6725 Szeged, Semmelweis u. 6, Hungary
[b] Department of Physical Chemistry and Materials Sciences, University of Szeged, H-6720 Szeged, Aradi v.t.1, Hungary
[c] MTA-SZTE Supramolecular and Nanostructured Materials Research Group, Department of Medical Chemistry, Faculty of Medicine, H-6720 Szeged, Dóm tér 8, Hungary
[d] Department of Health Economics, Faculty of Medicine, University of Szeged, H-6720 Szeged, Szőkefalvi-Nagy Béla u. 6, Hungary

ARTICLE INFO

Article history:
Received 10 December 2015
Received in revised form 15 February 2016
Accepted 23 February 2016
Available online 27 February 2016

Keywords:
Nanohybrid surface
Adhesion
Photooxidation
Antibacterial
Peptidoglycan
MRSA

ABSTRACT

The aim of this study was to develop photoreactive surface coatings, possessing antibacterial properties and can be activated under visible light illumination (λ_{max} = 405 nm) using LED-light source. The photocatalytically active titanium dioxide (TiO_2) was functionalized with silver nanoparticles (Ag NPs) and immobilized in polyacrylate based nanohybrid thin film in order to facilitate visible light activity ($\lambda_{Ag/TiO2,max}$ = 500 nm). First, the photocatalytic activity was modelled by following ethanol vapor degradation. The plasmonic functionalization resulted in 15% enhancement of the activity compared to pure TiO_2. The photoreactive antimicrobial (5 log reduction of cfu in 2 h) surface coatings are able to inactivate clinically relevant pathogen strains (methicillin resistant *Staphylococcus aureus*, *Escherichia coli*, *Pseudomonas aeruginosa*) within short time (60–120 min) due to the formed and quantified reactive oxygen species (ROS). The existence of electrostatic interactions between the negatively charged bacteria (from −0.89 to −3.19 μeq/10^9 cfu) and positively charged photocatalyst particles (in the range of +0.38 and +12.3 meq/100 g) was also proven by charge titration measurements. The surface inactivation of the bacteria and the photocatalytic degradation of the cell wall component were also confirmed by fluorescence and transmission electron microscopic observations, respectively. According to the results an effective sterilizing system and prevention strategy can be developed and carried out against dangerous microorganisms in health care.

1. Introduction

Interdisciplinary researches of nanotechnology and microbiology have become great interest to develop environmental applications against bacteria causing nosocomial infections [1–5]. *Staphylococcus aureus* (*S. aureus*) and *Pseudomonas aeruginosa (P. aeruginosa)* are common pathogenic bacteria with a possible multidrug resistance by mutation [6,7]. Immunosuppressed patients are compromised, these infections highlights the importance of prevention in the health care [8–11]. Methicillin resistant *S. aureus* and multidrug resistant *P. aeruginosa* can cause nosocomial infections and are responsible for postoperative infection. The number of infections caused by these bacteria is increasing in every year, so the prevention of the spread from human to human is the key to maximize the function of infection control. Antimicrobial applications are able to inactivate bacteria, viruses and fungi on different surfaces, in water or in the air, so they can be the main actor of prevention in the health care facilities [12–14]. There are various techniques to develop antimicrobial surfaces, but only a few optimize the structure and the chemical properties [15–20]. Surfaces with TiO_2 content can kill numerous microorganisms because of its photocatalytic properties [21–26]. Moreover, during photocatalysis under UV light illumination strong oxidizing power is generated and the surface containing TiO_2 shows antibacterial effect as well. In the course of photocatalysis different free radicals (*e.g.*, hydroxyl radicals) are also produced with different wavelength emitting light

* Corresponding author. Fax: +36 62 544 042.
E-mail addresses: i.dekany@chem.u-szeged.hu, i.dekany@sol.chem.u-szeged.hu (I. Dékány).

http://dx.doi.org/10.1016/j.apsusc.2016.02.202
0169-4332/

sources. [27,28]. Hydroxyl radicals can destroy the bacterial cell wall due to breaking covalent bonds in peptidoglycan layer, which is mainly responsible for the stability of the cell wall in Gram-positive (GR+) and Gram-negative (GR−) bacteria [29]. Due to the destruction of cell wall and DNA the reproduction and infectivity of the microorganisms can be inhibited in a short time period [30–34]. UV-active photocatalyst particles (*e.g.*, TiO_2, or ZnO) can be modified with different plasmonic nanometals, so the wavelength of the absorbing light can be tuned from the UV to the visible region. Due to this disinfection method a wide range of pathogen bacteria can be inactivated under visible light illumination [35–39]. The wavelength of the absorbing light on TiO_2 nanoparticles (NPs) can be extended to the visible region functionalizing with silver, without significant amount of silver ion release to the environment. The antibacterial activity and photochemical qualifications of TiO_2 photocatalysts and its modified forms have been reported in many publications, but the connection properties between the NPs and the bacterial cells are relatively unknown. Investigation of the bacterial adhesion on the surface of antibacterial NPs is very important [40,41]. It is already well-known, that the cell wall of bacteria are negatively charged because of the presence of teichoic acids for GR+ bacteria [42] while in case of GR− bacteria the presence of lipopolysaccharides and lipoproteins cause the negative charge and thus [43] they can be electrostatically attached to the positively charged surfaces of the applied photocatalysts. The knowledge of the surface charge values of the prepared antimicrobial surfaces may contributes to the better understanding of the successful inactivation of microorganisms.

In our work photoreactive surface coatings, possessing antibacterial properties have been developed and the adhesion properties of methicillin resistant *S. aureus* (GR+), *P. aeruginosa* (GR−) and *Escherichia coli (E. coli)* (GR−) were investigated on the surface of photoreactive nanohybrid films containing TiO_2 and plasmonic Ag–TiO_2 NPs in polymer matrix. In addition, the antibacterial activity of Ag–TiO_2 photocatalyst was also investigated. Our main goal was to highlight the connection between the bacterial adhesion and the antimicrobial properties of the developed nanohybrid films for possible application in health care.

2. Materials and methods

2.1. Preparation of polyacrylate hybrid films containing TiO_2 and Ag–TiO_2 photocatalyst

Degussa P25 TiO_2 (75% anatase, 25% rutile) was functionalized with Ag NPs. Different Ag NPs/TiO_2 ratios were tested, but according to the TiO_2 content 0.5 w/t% concentration of Ag NPs was applied [44]. During the synthesis the calculated amount of $AgNO_3$ aqueous solution (Molar, Hungary) was directly added to the TiO_2 aqueous suspension. On the second step the silver ions were reduced by one hour of irradiation with UV light (Hamamatsu L8251 lamp; $P = 150$ W; $\lambda_{max} \geq 300$ nm). The nanocomposites were washed four times, dried at 50 °C and pulverized [44]. For microbiological measurements the photocatalyst NPs were immobilized by using polyacrylate [poly(ethyl-acrylate *co* methyl-methacrylate) (p(EA-*co*-MMA)) binder material (obtained from Evonik Industries, Germany). Photocatalyst NPs in polymer matrix were prepared on the surface of glass plates (2.5×2.5 cm) with spray coating technique. The amount of the nanohybrid surface coating deposited on the glass plates was 1 ± 0.1 mg cm^{-2} in all cases. The concentration of the photocatalyst in the composite film was 0.6 mg cm^{-2} which corresponds to the photocatalyst/polymer mass ratios of 60:40 wt%. The calculated thickness of these films was 1.48 ± 0.1 μm [45]. Pure polymer matrix was also prepared in the same manner for reference.

2.2. Characterization of the nanohybrid surfaces

Diffuse reflectance spectra of the photocatalysts were recorded with CHEM 2000 UV–vis (Ocean Optics Inc.) spectrophotometer [44,45]. The photocatalytic activity of the polyacrylate based nanohybrid films and the pure photocatalysts thin layer (without polymer binder) were performed with the ethanol (as test molecules) degradation test under LED-light illumination (General Electric's, Hungary, $\lambda = 405$ nm) [44]. Photooxidation of ethanol vapor on catalyst films was performed in a circulation reactor (volume *c.a.* 165 mL) at 25.0 ± 0.1 °C. The light source was fixed at 50 mm distance from the 45 cm^2 films. After injection of ethanol and water vapor, the system was left to stand 30 min for the establishment of adsorption equilibrium on the surface of films. The composition of vapor phase was analyzed by gas chromatograph (Shimadzu GC-14B) equipped with a thermal conductivity (TCD) and a flame ionization detector (FID). The flow rate of the gas mixture in the photoreactor system was 375 mL × min^{-1}. The initial concentration of the ethanol was 0.36 ± 0.018 mmol L^{-1} at relative humidity of ~70%. During the long- term photocatalytic test experiments of the Ag–TiO_2 containing nanohybrid film the 45 cm^2 layer was illuminated continuously with $\lambda = 405$ nm LED light from a distance of 10 cm. At given time intervals the irradiated hybrid layer was put in the above described circulation reactor and the photooxidation rate of ethanol vapor was measured. After the measurement the specific amount of photodegraded ethanol (Δc_{EtOH}/mM 60 min^{-1} g^{-1}/) was calculated. The surface pH of the Ag–TiO_2 containing polymer based nanohybrid film was determined under UV-light illumination (GCL307T5VH/HO type low-pressure mercury lamp, LightTech, Hungary, $P = 35$ W). During the measurement the 5×5 cm^2 nanohybrid film was immersed in 40 mL of distilled water (initial pH 5.3 due to the dissolved CO_2). The nanohybrid films were illuminated and shaken continuously during the experiment with a magnetic stirrer. The distance of the light source from the nanohybrid films was 10 cm. The pH electrode (Metrohm 6.0228.010) was placed into the distilled water nearest to the hybrid film and the actual pH values were measured as a function of illumination time.

2.3. Surface charge measurements

Surface charge values of the photocatalyst and the bacterial suspensions were measured by means of a particle charge detector (PCD-04 Particle Charge Detector; Mütek Analytic GmbH, Germany) with manual titration. Under a titration process the surface charge of the bacteria and photocatalysts will be compensated with opposite charged surfactants like: sodium dodecyl sulfate (SDS) and hexadecylpyridinium chloride (HDPCl) with concomitant streaming potential measurements. 10 mL of 0.1% TiO_2 suspension was measured in the particle charge detector at pH 4.5, because the optimal pH of the three investigated bacteria is in the range of $4.2 \leq pH \leq 9$ and TiO_2 is positively charged below pH 6 (point of zero charge) [46]. Photocatalyst and bacterial suspensions were titrated with anionic 1% SDS and cationic 0.01% HDPCl solutions, respectively. In view of the amount of the added surfactant at the charge compensation point (streaming potential = 0 mV) the equimolar amount of surfactant was calculated and specified to the amount of photocatalyst (meq/100 g) or to the number of bacteria (μeq/10^9 cfu). All experiments were repeated in three times.

2.4. Determination of the produced hydroxyl radicals on the nanohybrid films

The amount of reactive hydroxyl radicals was determined from the hydrogen peroxide induced luminol dependent chemiluminescense reaction (Scheme 1.) The detailed measurements

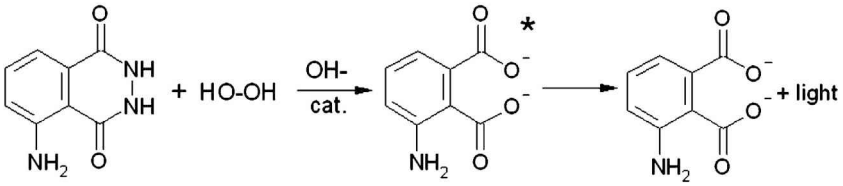

Scheme 1. The hydrogen peroxide induced luminol dependent chemiluminescense reaction.

were described in our previous publication [45]. Briefly, $5 \times 5\ cm^2$ nanohybrid films were immersed in 40 mL distilled water and illuminated with LED-lamp ($\lambda = 405$ nm) under continuous shake. The distance of the light source from the nanohybrid films was 10 cm during the measurement. 100 μL samples were taken after 2.5, 5, 10, 20, 30, 60 and 120 min of illumination time and added to 100 μL of luminol solution ($c_{luminol} = 33.8$ mM) and the intensity of the chemiluminescense (CL) was measured immediately by the Sirius L luminometer. Based on the previously determined calibration curve, the concentration of the formed hydroxyl radicals is directly proportional with the measured relative light unit (RLU) values as follows:

$$C_{H_2O_2} = \frac{\text{Relative light unit}\left(\frac{RLU}{s}\right)}{41866} \quad (1)$$

For quantitative characterization of the free radical concentration from the RLU data the calculated concentration of H_2O_2 (mM) are displayed as the function of illumination time. Data were compared to the CL values of pure polymer films and to luminol with distilled water.

2.5. Preparation of bacterial suspensions

E. coli ATCC 29522, *P. aeruginosa* ATCC 27853 and methicillin resistant *S. aureus* ATCC 43300 (reference strains obtained from international reference culture collection) were used as the test strains for the microbiological measurements and microscopic examinations. Bacteria were grown on the surface of Brain Heart Infusion agar (BHI-agar, Oxoid supplemented with 5% cow blood). Cultures were incubated statically under aerobic conditions for 24 hours at 37 °C. Isolated colonies were suspended in 5 mL Brain Heart Infusion broth (BHI-broth, Oxoid, Hampshire, UK). Bacterial suspensions were prepared in physiological saline ($c_{NaCl} = 0.9$ wt%) and the concentration of the bacterial suspensions were adjusted to $1 \times 10^5 - 5 \times 10^5$ cfu/mL, which was calculated from the optical density (absorbance at 600 nm; OD_{600}). The optical density was determined by using UVIKON 930 spectrophotometer (Kontron Instruments, Germany). Optical density data were supported with counting colony forming units in a serial dilution (to 10^{-7}) at the logarithmic phase with BZG 40Colony Counter (WTW GmbH, Germany).

2.6. Fluorescence microscopy and fluorometric measurements

For the fluorescence microscopy and fluorometric investigations *P. aeruginosa*, *S. aureus* and *E. coli* bacteria were used. All of the investigated bacteria were grown on nutrient agar (Mueller-Hinton) in logarithmic phase according to the user's guide of the viability kit (LIVE/DEAD® *Bac*Light™ Bacterial Viability kit L7007, Life Technologies, Hungary). After the process of the photocatalysis experiment, surviving bacteria were washed out from the nanohybrid film with three milliliters of physiological saline. During the fluorometric studies and fluorescence microscopy 6 μL of the dye mixture was added for each mL of bacterial suspension ($1 \times 10^5 - 5 \times 10^5$ cfu/mL) and incubated for 20 min in room temperature in dark conditions [47,48]. In the staining kit fluorescence dyes are in a mixed, two component formulation. Syto 9 can penetrate to the bacterial cell wall and labels both the live and dead bacterial cells. Propidium iodide (PI) has no ability to penetrate the live bacterial cell wall, only when it is damaged resulting in the decrease in the SYTO 9 stain fluorescence, when both dyes are labeling bacteria. The adhesion of bacteria on photocatalyst particles was observed with light microscope (Leica DM IL LED Fluo). The viability of the cells was controlled with fluorescence microscopy equipped with L5 and N2.1 filter systems (Leica Microsystems, Germany) [48,49]. The bactericidal activity of the films was proved with fluorometric measurements, which were carried out with spectrofluorometer (Fluoromax 4, Horiba-Yvon-Joben). The reduction (R%) of bacteria after different time of illumination on the nanohybrid films was measured from the intensity (I) of fluorescence emission at 500 – 510 nm in case of Syto 9 and at 600 – 630 nm in case of PI. After several fluorometric investigations the wavelength of the excitations were optimized; Syto 9 (16.7 mM) and propidium iodide (16.7 mM) dyes were excited by 470 nm with the spectrofluorometer. The emission peaks were read at ~500 nm by Syto 9 and at ~620 nm by propidium iodide, respectively. The antibacterial activity (*R*%) was calculated according to the Eq. (2) [49].

$$R\% = \frac{(I - I_0)}{I_0} \times 100 \quad (2)$$

I_0 is the fluorescence emission of the initial (untreated) bacterial suspension containing the above mentioned selective dyes (read at 500–520 nm) and I is the fluorescence emission at the same wavelength after 120 min of illumination of LED-light source. Integrated intensities of the green (510–540 nm) and red (620–650 nm) emission were recorded, and the green/red fluorescence ratios ($Ratio_{G/R}$) were calculated according to the Eq. (3).

$$Ratio_{G/R} = \frac{F_{cell,em1}}{F_{cell,em2}} \quad (3)$$

2.7. Preparation of the bacterial cell wall component for TEM microscopy

The structure of peptidoglycan (sacculus) of *S. aureus* (obtained from Sigma–Aldrich, USA) and *E. coli* (prepared in our laboratory) was investigated during photocatalysis process under different time of illumination. *E. coli DH5α* was maintained and cultured in Luria-Bertani (LB) broth with vigorous shaking at 37 °C. Eighty milliliter of the cell culture was centrifuged for 20 min with 2500 rpm at room temperature. The supernatant was removed, and the sediment was suspended in 10 mL distilled water and 10% SDS was added to give a final concentration of 4%. The suspension was poured into a plastic tube (50 mL), which was boiled in a glass beaker for 4 h, keeping the water level on 250 mL and after was cooled and incubated for overnight at room temperature continuing the stirring. Seventy milliliter of the suspension was centrifuged at 14000 rpm for one hour, the supernatant was removed. The resulting suspension was dialyzed against 10 mM Tris/HCl (pH 7.2) [10]. The prepared samples were examined in different dilutions (100×; 1000×; 10000×) [50]. At the initial point of the investigations 0.1 mL of peptidoglycan suspension

(25 mg mL^{-1}) was added in a microtiter plate to 0.1 mL suspension of silver functionalized TiO_2 (0.5 mg mL^{-1}) photocatalyst. During the experiment the photocatalyst/peptidoglycan mixture was illuminated with LED-light source (λ = 405 nm) for different times (60 and 120 min). Peptidoglycan suspension without photocatalyst particles was investigated for reference. Samples were loaded on one-hole grids with immersion method. The effect of silver functionalized TiO_2 to the peptidoglycan structure was observed on peptidoglycan layer of the cell wall of *S. aureus* and *E. coli* with Philips CM10 electron microscope (magnification: 13500×).

2.8. Antibacterial measurements

The antibacterial tests were carried out according to modified EN ISO 27447:2009 standard. For the evaluation of the surviving bacteria the washing technique was used, because the counting of the survival bacteria is more accurate with this method [45]. Before the microbiological measurements nanohybrid films on glass samples were activated by UV-irradiation for an hour (light source: LightTech GCL307T5L/Cell lamp λ = 250 nm) to increase the concentration of the photocatalyst particles in the surface region of the nanohybrid films [45]. $1 \times 10^5 - 5 \times 10^5$ cfu/mL bacterial suspensions were spread uniformly (0.1 mL) on the surface of the nanohybrid films (2.5×2.5 cm^2) and covered with the top of Petri dish during the experiment, to avoid water vapor evaporation which can modify results [45]. During the microbiological measurements the glass samples with the nanohybrid films were illuminated with visible-light (light source: LED lamp 7W; λ = 405 nm), exposure times were 0, 30, 60, 90 and 120 min. During the experiments the distance of the light source from the nanohybrid films was 35 cm [51]. The light intensity of the LED-light source on the surface of the nanohybrid films was measured with a power meter (Thorlabs GmbH, Germany). After different illumination periods the inoculated nanohybrid films were placed into a new sterile Petri-dish by sterile tweezers and the inoculums were washed out from the activated nanohybrid films with 3 mL sterile physiological saline water to regain all surviving bacteria from the uneven surface of the samples [51]. Bacterial suspensions with survival bacteria were streaked (0.1 mL) uniformly on the Mueller-Hinton (Oxoid, Hampshire, UK) media. After the incubation time (37 °C; 24 h) the antibacterial activity was evaluated by counting colony forming units (cfu/mL) with BZG40Colony Counter (WTW GmbH, Germany). The number of colony forming units were converted to the cell number of the survival bacteria per milliliter of the original inoculums on the nanohybrid films. The antibacterial efficiency was calculated from the Eq. (4):

$$R\% = \frac{(N - N_0)}{N_0} \times 100 \quad (4)$$

where $R\%$ is the percent of inactivation of live bacteria, N_0 is the initial concentration of live bacteria and N is the concentration of bacteria after different illumination times on nanohybrid films.

2.9. Statistical analysis

All values are expressed as means ± S.D. Standard deviations were calculated from three parallel antibacterial experiments. Significant differences between groups were compared and calculated with One-way ANOVA Tukey *Post-hoc* test. Differences between groups were considered significant at $p < 0.05$ [52].

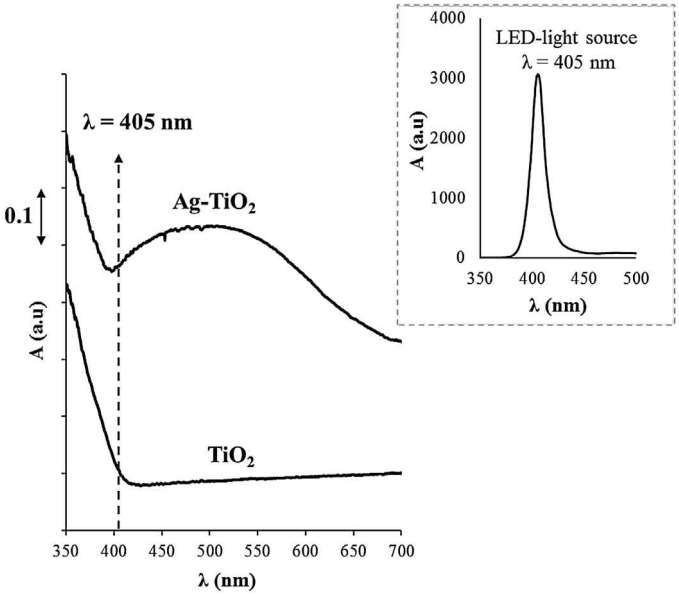

Fig. 1. Diffuse reflectance spectra of TiO_2 and Ag–TiO_2 photocatalyst thin films (1 ± 0.1 mg cm^{-2}) and the emission spectra of the LED-light source (λ = 405 nm) (inset).

3. Results

3.1. Characterization of the nanohybrid films with TiO_2 and Ag–TiO_2 photocatalyst content

TiO_2 and Ag–TiO_2 were successfully immobilized in p(EA-*co*-MMA) polymer layer and prepared on glass holders for antibacterial, toxicity and fluorometric tests. The synthesized nanohybrid films are mechanically stable and showed enhanced short-time antibacterial effect. Diffuse reflectance spectra verifies the presence of Ag NPs on the TiO_2 particles. Due to the surface modification with Ag NPs, the UV–vis spectrum of the originally white P25 TiO_2 was changed: the Ag–TiO_2 showed a broad visible absorption band at λ_{max} = 500 nm which is unambiguously attributed to the plasmonic absorption of Ag NPs (Fig. 1.). In the noble metal–semiconductor composite photocatalysts, the noble metal NPs act as a major component for harvesting visible light due to their surface plasmon resonance while the metal–semiconductor interface efficiently separates the photogenerated electrons and holes. The photocatalytic efficiency of the reactive TiO_2 and Ag–TiO_2 photocatalyst thin layers were evidenced by photooxidation measurements and compared to the photocatalytic effect of Ag–TiO_2 in polymer matrix (Fig. 2.). Before the photocatalytic and microbiological measurements the nanohybrid films were activated by UV-irradiation for an hour (light source: LightTech GCL307T5L/Cell lamp λ = 250 nm) to increase the concentration of the photocatalyst particles in the surface region of the hybrid films [45]. In our previous work the wetting properties of the polymer based hybrid photocatalyst layers were investigated by contact angle measurements in order to prove this photocatalyst surface accumulation [44]. We found that the initial contact angle values were 27 and 14° in the case of TiO_2 and Ag–TiO_2 containing hybrid layers, respectively. During the one hour UV- irradiation the measured contact angle values were rapidly decreased to 2° (TiO_2) and 0.5° (Ag–TiO_2). The reason for this is that the polymer matrix was photodegraded during the irradiation, so the hydrophilic photocatalyst particles become free from upper polymer layer resulting lower contact angle values (so-called light razor effect) [44]. Fig. 2 clearly represents that the 45 cm^2 Ag–TiO_2 thin film can degrade more ethanol (~95% of the initial 0.36 mM) after 60 min LED-light

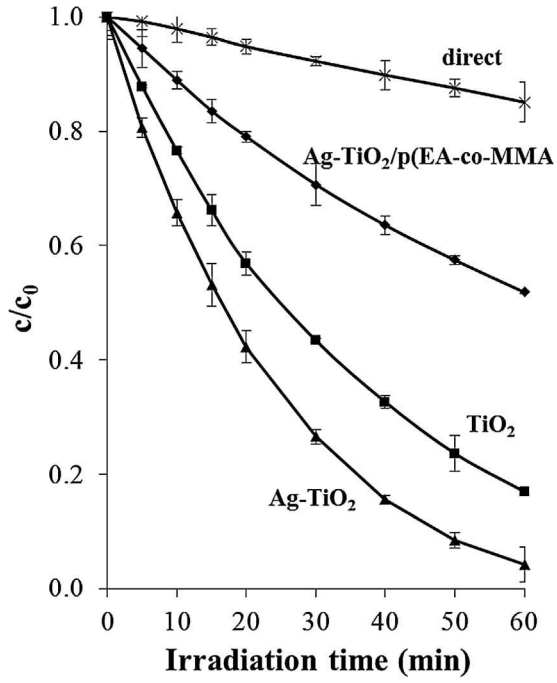

Fig. 2. Photooxidation of the ethanol on different nanohybrid films (pure TiO_2, Ag–TiO_2 and Ag–TiO_2/polymer coated surfaces) in photoreactor at different illumination time using LED-light source ($\lambda = 405$ nm; $t = 60$ min).

($\lambda_{max} = 405$ nm) illumination time than the pure TiO_2 (~80% of the initial ethanol concentration). This is due to the enhanced visible light activity of the noble metal functionalized Ag–TiO_2 photocatalyst. Incorporation of the photocatalysts particles into the polymer matrix resulted in a drastic decrease (48% of the initial 0.36 mM ethanol) in the photocatalytic reaction rates, compared to pure Ag–TiO_2 (~95% of the initial ethanol concentration), since the polymer partially covered the photocatalyst particles and interfered with the photocatalytic degradation of model pollutant (Fig. 2). It can be concluded that the application of polymer matrix was reduced the photocatalytic activity of the embedded Ag–TiO_2 particles, however, according to our previous results, the prepared polymer films showed very good mechanical stability [44]. According to the previously presented adhesive tape test the polymer firmly bound the catalyst NPs; thus, minor amount of particles could be removed by the tape from the surface.

Our next question was how the above mentioned polymer partially photodegradation affects the long-term photocatalytic activity of the nanohybrid layers. Fig. S1 shows the long-term photocatalytic activity of polymer based photocatalyst thin layer containing immobilized Ag–TiO_2 photocatalyst particles. At the beginning of the 405 nm LED light illumination the measured values are increased compared to the initial value ($\Delta c_{EtOH} = 0.022$ mM 60 min^{-1} g^{-1}) of the film. This is due to the polymer photodegradation and the increasing number of surface photocatalyst particles. This is also confirmed by AFM measurements in our previous paper [44]. After 192 h (8 days) LED light illumination the measured photocatalytic values were shown a local maximum ($\Delta c_{EtOH} = 0.0283$ mM 60 min^{-1} g^{-1}) and next decreased continuously during the long term illumination time. After seventeen thousand hour (that means almost two years continuous LED light illumination) the measured photocatalytic value ($\Delta c_{EtOH} = 0.0092$ mM 60 min^{-1} g^{-1}) was about half of the initial value. So, according to the results, it can be concluded, that in spite of the polymer matrix partially photodegradation, the nanohybrid photocatalyst films preserve their photoreactivity.

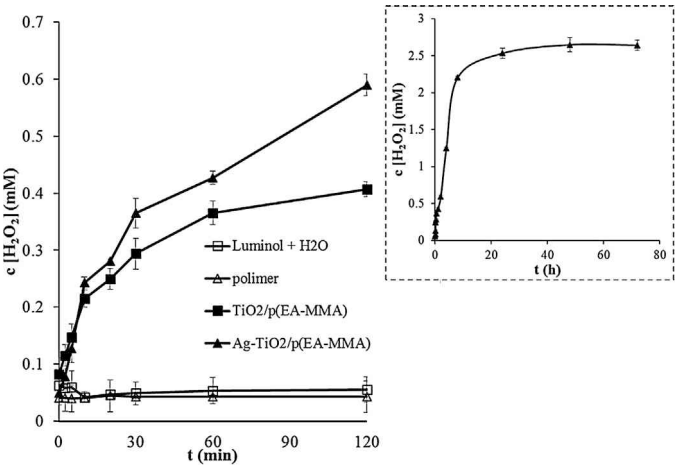

Fig. 3. Characterization of the formation of free radicals on different surfaces via RLU chemiluminescense intensity measurements. Representation of the equivalent H_2O_2 concentration as a function of illumination time (0–120 min) using LED-light source ($\lambda = 405$ nm). The inset shows the results for a long-time period (only for Ag–TiO_2/polymer nanohybrid film).

3.2. Determination the amount of reactive hydroxyl radicals

During the process of photocatalysis under appropriate (exciting) wavelength reactive hydroxyl radicals (OH•) are produced, which are primarily responsible in inactivating bacteria [47]. Hydroxyl radical is the most reactive oxygen species and cause irreversible DNA degradation in bacteria [47]. The amount of OH• produced on the nanohybrid films under photocatalysis was calculated from the reaction of H_2O_2 and luminol. The detailed method of the measurement was presented in a previous publication [45]. The lifetime of the free radicals can be measured in femto- or picoseconds [53]. The degradation of hydrogen peroxide (which is produced from OH•) is slow in room temperature; therefore, it can be measured with a luminometer [54]. For quantitative characterization of the free radical concentration from the RLU data, the calculated equivalent concentration of H_2O_2 (mM) is displayed as the function of illumination time with a LED light source. CL intensity was converted in equivalent H_2O_2 concentration after a calibration process using 0.1–5.0 mM H_2O_2 solutions. The determined calibration curve (Fig. S2) presents that the adjusted H_2O_2 concentration is proportional to the measured RLU intensity values. Results showed that after 30 min illumination there is an increase of producing radicals even on TiO_2/polymer and Ag–TiO_2/polymer nanohybrid films compared to the control (the polyacrylate thin layer without photocatalyst) measurements (Fig. 3). In accordance to the previously presented photocatalytic test results, the amount of the produced OH• is higher on the surface of Ag–TiO_2/polymer nanohybrid film (0.33 mM H_2O_2 equivalent), than in the presence of TiO_2/polymer (0.24 mM H_2O_2 equivalent) after 20 min under visible light illumination. After 120 min of illumination the increase of the amount of OH• is slowing on TiO_2/polymer nanohybrid film, a saturation curve can be seen on the pattern (~0.4 mM H_2O_2 equivalent after 120 min). On the surface of Ag–TiO_2/polymer nanohybrid film the increase of OH• radical concentration is slowing only after 48 h and continues in a saturation curve of the produce (Fig. 3 inset). This slowly increasing and saturated radical production is due to the previously reported partially photodegradation of polymer binder material. In our previous work it was demonstrated that the photoaging significantly improved the photocatalytic activity of the photocatalyst containing nanohybrid films. It was presented that the longer time the treatment lasted, the better photocatalytic efficiencies were attained for the hybrid films [44]. Due to this phenomenon the concentration of the photocatalyst particles on

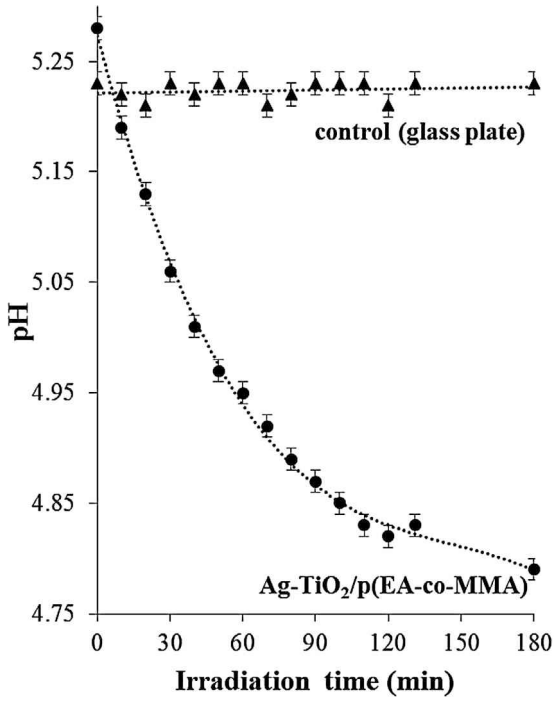

Fig. 4. The measured surface pH values of the Ag–TiO_2/polymer thin hybrid layer as a function of irradiation time.

the surface region is increased, so bacterial cells can directly connect to them [45]. This observation is in good agreement with the presented H_2O_2 equivalent concentration values.

3.3. Surface charge and pH measurements

Before the surface charge measurements the relevant pH of the polyacrylate based hybrid layer containing Ag–TiO_2 NPs was determined. The pH has determinant role because the surface charge of the TiO_2 depends on the environmental pH [46]. According to the different publications, TiO_2 is positively charged below pH 6 (point of zero charge) [55]. Fig. 4 shows the measured pH values as a function of UV-irradiation time. At $t = 0$ min the initial pH was 5.27 and during the UV-illumination it was found that the pH values were continuously decreased. After 180 min, the measured pH reached the pH 4.8 according to the formation of reactive radicals. Based on the above mentioned results, the relevant pH of the photocatalyst containing hybrid layer was slightly acidic, so the charge titration measurements were carried out at pH 4.5. Surface charge of the photocatalysts and bacteria was calculated from the streaming potential data in each case. Fig. 5A shows the measured streaming potential of 10 mL 1% TiO_2 suspensions titrated with 1% SDS solution at pH 4.5. The streaming potential induced in the TiO_2 aqueous suspension was positive at this pH, then it continuously decreased due to progressive deprotonation of $TiOH_2^+$ surface sites and the concomitant loss of surface charge. Considering the added amount of the charge compensating surfactant molecules ($n_{SDS} = 0.0123$ mmol) and the mass of the measured TiO_2 ($m_{TiO2} = 0.1$ g), the specific surface charge of TiO_2 NPs was +12.3 meq/100 g at pH 4.5 [specific charge = $c_{SDS} \times V_{SDS}/m_{TiO2}$]. Similar to pure TiO_2 the Ag–TiO_2 was also titrated and +0.38 meq/100 g value was obtained. Fig. 5B represents the measured streaming potential of 10 mL 1.09×10^7 cfu/mL *E. coli* bacteria suspensions titrated with 0.01% HDPCl solution at the same pH. In this case the charge titration curve shows opposite effect: the initial bacterial suspension has negative streaming potential and it continuously decreases due to the increasing amount of positively charged surfactant molecules. The determined specified charge of *E. coli* bacteria was −1.33 μeq/10^9 cfu, while −3.19 μeq/10^9 cfu and −0.89 μeq/10^9 cfu values were determined for *P. aeruginosa* and MRSA, respectively. The measured negative charge corresponds to the presence of teichoic acid groups embedded in bacterial peptidoglycan cell wall component in case of GR+ bacteria. For GR− bacteria the presence of the polysaccharide chains embedded in peptidoglycan cell wall component cause the negative charge [42,43]. In view of the specific surface charge values, 10 mL 1.09×10 cfu/mL *E. coli* bacteria suspension was titrated with 1% TiO_2 suspension which is presented in Fig. 5C. According to the titration curve, 10^9 cfu *E. coli* bacteria can be bonded by adhesion of 1.88 g TiO_2 particles. Table 1 summarizes the determined surface charge values of the applied photocatalyst (TiO_2 and Ag–TiO_2) and the studied bacteria as well. The results clearly shows that, the GR− bacteria (*E. coli* and *P. aeruginosa*) showed higher surface charge values than the GR+ (*S. aureus*) bacteria. It was established that, *P. aeruginosa* has the highest surface charge

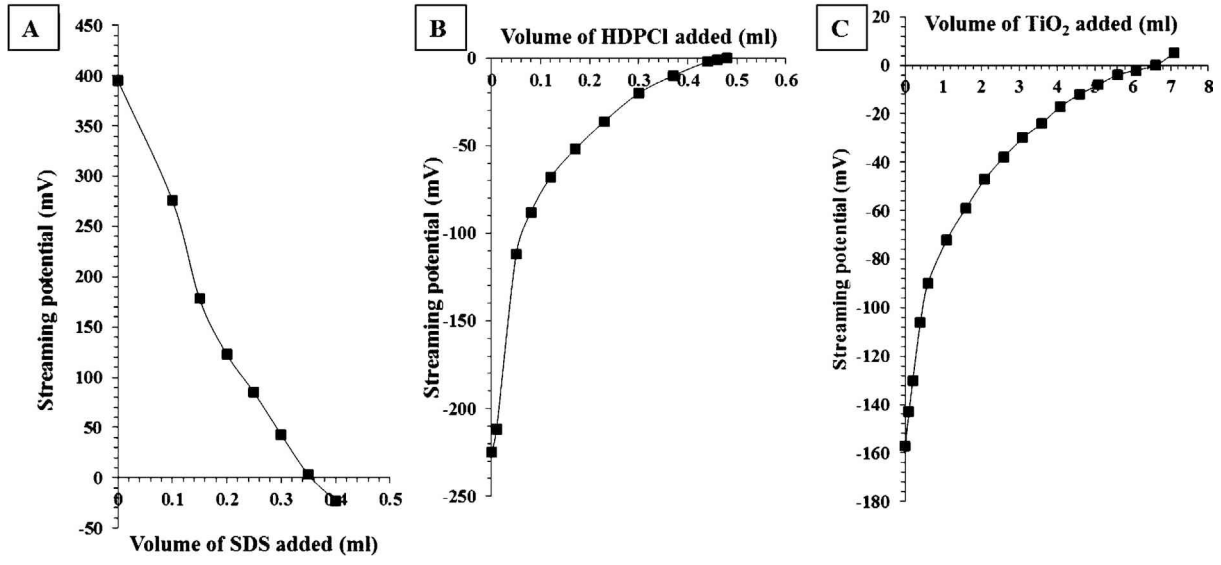

Fig. 5. Determination of the specific surface charge values for TiO_2 (A), for *E. coli* bacteria (B) and the amount of the adhered TiO_2 on the surface of *E. coli* at the electrostatic charge compensation point (C). In all cases the pH was 4.5 and the standard error is 2.0%.

Table 1
The calculated surface charge values of the applied photocatalysts and the studied bacteria.

Photocatalysts or bacteria	Concentration	Measured surface charge (at c.e.p.)[a]	Calculated surface charge[b] (coulomb/10^9 cfu)	Electrostatically adhered TiO_2 (g/10^9 cfu)
TiO_2	1%	+12.3 meq/100 g		
Ag–TiO_2	1%	+0.38 meq/100 g		
E. coli (GR−)	1.06×10^7 cfu/mL	−1.33 μeq/10^9 cfu	0.129	1.88
P. aeruginosa (GR−)	1.32×10^7 cfu/mL	−3.19 μeq/10^9 cfu	0.308	2.55
MRSA (GR+)	1.09×10^7 cfu/mL	−0.89 μeq/10^9 cfu	0.086	0.61

[a] Specified surface charge (c.e.p.) = $c_{surfactant} \times V_{surfactant}/m_{TiO2or\ bacteria}$.
[b] Calculated surface charge (coulomb/10^9 cfu) = ($n_{added\ surfactant}$ × Faraday constant)/number of bacteria.

(−3.19 μeq/10^9 cfu) and it adhered the highest amount of TiO_2 (2.55 g TiO_2/10^9 cfu). According to the results, it can be also concluded that between the negatively charged bacteria and positively charged photocatalyst particles electrostatic interactions also exist at the relevant pH value (~4.5).

3.4. Studies of the cell wall stability by fluorescence microscopy and fluorometric measurements

These emerging electrostatic interactions between the Ag–TiO_2 particles and the investigated bacteria were also confirmed by microscopic observations. Bacterial suspensions of *E. coli* were stained with LIVE/DEAD® *Bac*Light™ staining kit. The samples were investigated at the initial point of the experiment (left images) and after 120 min (right images) of illumination with LED-light source as well. It was found that for *E. coli* at the initial point the live bacteria are strongly attached to the spherical Ag–TiO_2 aggregates and green emission (Fig. S3.A, left) was observed. After 120 min no green emission was detected (Fig. S3.A, right). In contrast, after 120 min of LED light illumination only the bacteria with damaged membrane (Fig. S3. B, right) can be seen on the surface of the photocatalyst particles and red emission was detected. In this case at 0 min (Fig. S3.B, left) this red emission is not seen. In the case of MRSA, *P. aeruginosa* and *E. coli* the fluorescence ratios of the live and the dead bacteria were calculated from the emission values at the above mentioned points (Fig. 6A). The emission changes of the live/dead bacteria were also confirmed by fluorometric measurements. Namely, the emission peaks were shown at ~500 nm by Syto 9 (live bacteria) and at ~620 nm by propidium iodide (dead bacteria), respectively. On Fig. 6B it can be seen, that only the fluorescence intensity of Syto 9 decreases measurable, because of the FRET-mechanism by propidium iodide [56,57].

3.5. Degradation effect of silver functionalized TiO_2 on bacterial peptidoglycan layer

The structure-degradation effect of Ag–TiO_2 photocatalysts was observed on the major component of the *E. coli* (Fig. 7) and MRSA (Fig. 8) cell wall after 0, 60 and 120 min of illumination with LED-light source. Peptidoglycan (also called murein) is a typical component of the bacterial cell wall, which is responsible for the rigidity of the bacterial cell wall, located outside of the cytoplasmic membrane. The cell wall of the GR+ bacteria (MRSA) is thick and the peptidoglycan layer constitutes almost 95% of the cell wall, instead of the cell wall of GR− bacteria (*E. coli*) with 5–10% of the peptidoglycan content [58,59]. A significant degradation can be seen on the surface of the sacculi after 60 min of illumination (Figs. 7 E and 8 E). After 120 min sacculi were totally degraded, the formation of peptidoglycan cross links are totally inhibited because of the presence of free radicals which were produced during the process of the photocatalysis (Figs. 7 F and 8 F). When sacculi without photocatalysts were observed there was no degradation in sacculi even after 120 min of illumination with LED-light source (Figs. 7 B and C; 8 B and C). According to this experimental results, the determinant effect of the Ag–TiO_2 photocatalyst has been proven on the peptidoglycan layer under visible light illumination in case of GR+ and GR− bacteria.

3.6. Photocatalytic effect of the hybrid layers on reproduction of bacteria

The antibacterial effect of the synthesized Ag–TiO_2 in p(EA-*co*-MMA) layer was presented by testing against three pathogen bacteria as well. Namely, *E. coli*, *P. aeruginosa* and *S. aureus* were examined according to the modified national standard ISO 27447:2009. The scheme of the antibacterial tests have already been presented in our previous publication [45]. During the tests on the nanohybrid films 0.4 mW cm^{-2} light intensity was applied, which is not antibacterial itself, according to the ISO 27447:2009 standard.[1] During the measurements the antibacterial efficiency (*R*%) was determined as a function of illumination time. From statistical data (Figs. 9–11) it is clearly seen that there was statistically significant difference ($P < 0.05$) between the antibacterial effect on Ag–TiO_2/polymer nanohybrid films compared to the absolute (glass plate) and relative (polymer binder without photocatalyst) controls after 60 min of visible light illumination (Figs. 9, 10 and 11). In accordance with the experimental results substantially stronger bactericidal effect was obtained on TiO_2/polymer and on Ag–TiO_2/polymer films under LED illumination in contrast to the dark controls for MRSA and *E. coli* (Figs. 9 and 11). This observation clearly support that the visible-light photocatalysis play a leading role in the inactivation of bacteria instead of the disinfectant property of silver (Figs. 9 and 11). There was no significant difference between the experiments in the dark and experiments under LED-light illumination when only polymer and blank films were used (Figs. 9–11). Based on this experiment it can be concluded, that the LED-lamp emitting at 405 nm has no effect on the bacterial growth under the applied 0.4 mW cm^{-2} light intensity. In case of *P. aeruginosa* no significant difference between experiments in the dark and under illumination was obtained (Fig. 10), because *P. aeruginosa* has an increased sensitivity against silver [60]. In order to confirm this assumption a silver ion release test have been performed in our previous publication by using potentiometric measurements [45]. We found that the silver ion concentration released from p(EA-*co*-MMA) based Ag–TiO_2 composite film was ~0.14 ppm after 1 week of immersion. This value is under the level of inhibitory effect of silver to bacteria [61,62]. The *S. aureus* was the most sensitive bacteria on TiO_2/polymer nanohybrid film after 60 min of illumination time. Moreover, the highest antibacterial activity against all of the investigated bacteria was established on Ag–TiO_2/polymer nanohybrid films using 90 min of illumination with LED light.

[1] Antibacterial for UV_A only > 0.5 mW cm^{-2}.

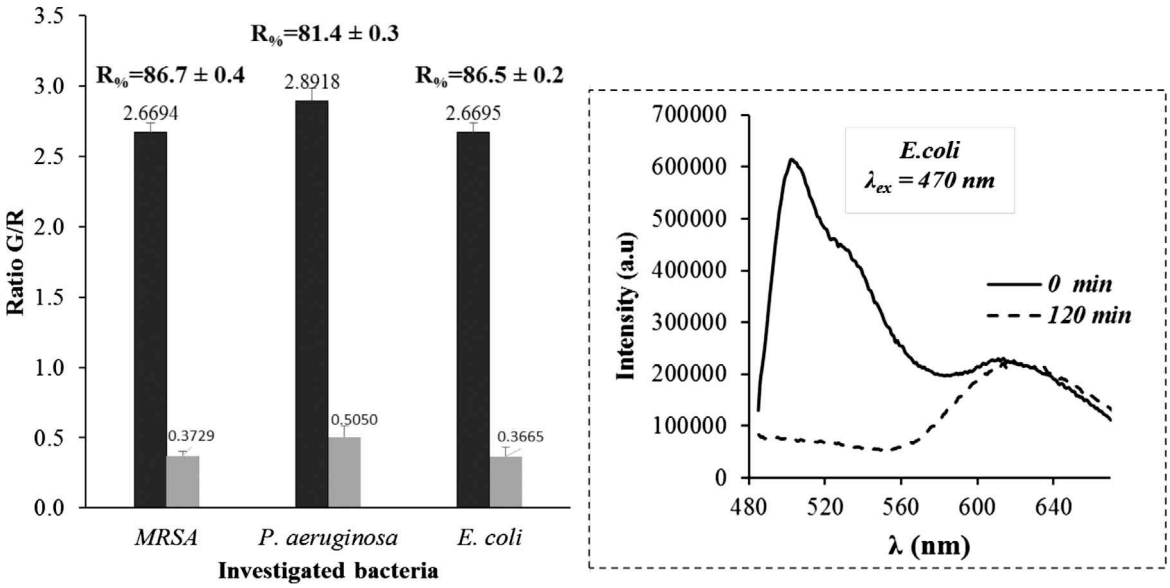

Fig. 6. Fluorescence ratio of the live/dead bacteria calculated from emission values at the initial point and after 120 min of illumination for MRSA, *P. aeruginosa* and *E. coli* (A); Fluorometric measurements of stained bacteria with Baclight© viability at the initial point and after 120 min of illumination in case of *E. coli* (B) (Propidium-iodide: λ_{ex} = 470 nm; λ_{em} = 610–650 nm; Syto9: λ_{ex} = 470 nm λ_{em} = 495–530 nm).

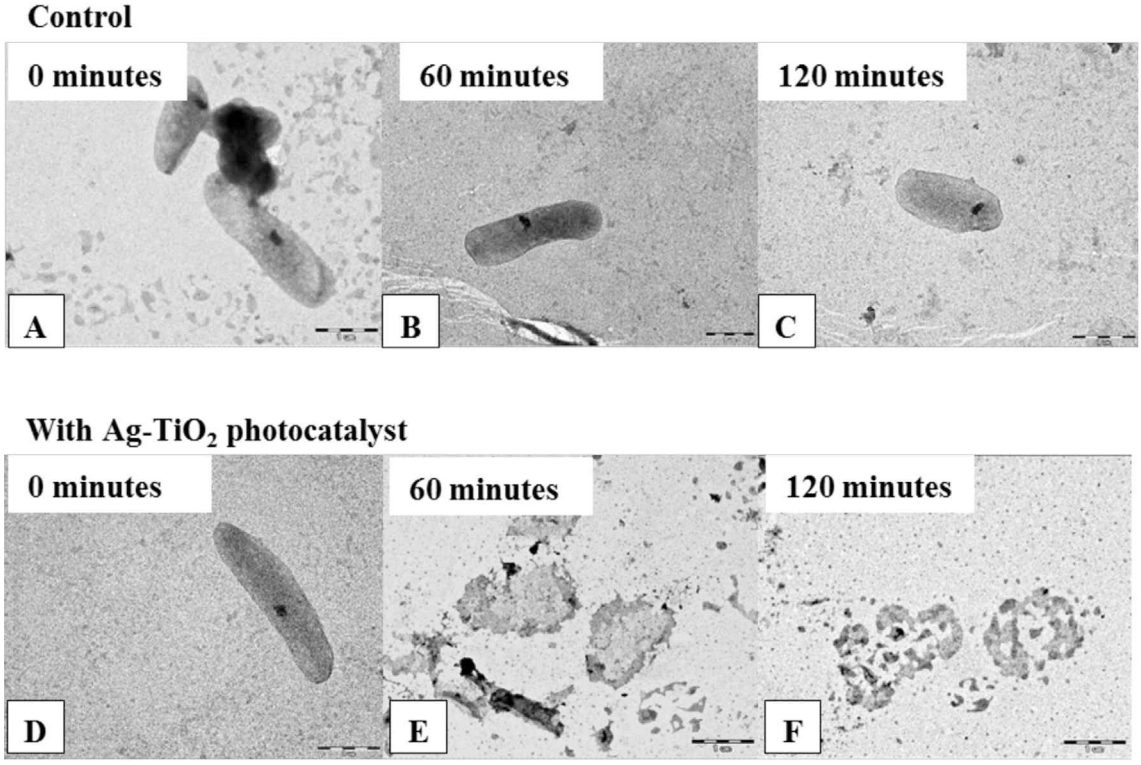

Fig. 7. Representative TEM images of the sacculi of *E. coli*; before reaction (A), after 60 min (B) and 120 min (C) of only visible light photocatalysis under illumination with LED-light source (λ = 405 nm) as control measurements and after 0 (D), 60 (E) and 120 min (F) on Ag–TiO_2 photocatalyst under the same conditions.

4. Discussion

This work demonstrate the photoreactive and antibacterial effects of nanohybrid films in four relevant steps. The first step highlights the adhesion properties of the negatively charged GR+ and GR– bacteria on the surface of the positively charged photocatalysts covered nanohybrid thin films. The second step demonstrates the degradation of the outer membrane of the studied bacteria via photocatalysis as a function of time through fluorescence staining method with LIVE/DEAD® *Bac*Light™ staining kit. Third step place emphasis on the degradation of peptidoglycan as a dominant component of cell wall, which is mainly responsible of the rigidity of the cell wall in the basis of TEM observations. In the last step the inhibition of reproduction of three pathogen bacteria was presented via the measurements according to modified ISO 27447:2009 standard. Because of the presence of carboxyl groups in the cell wall of the GR– bacterial cell, higher surface charge density was obtained than in the case of GR+ MRSA. It was also

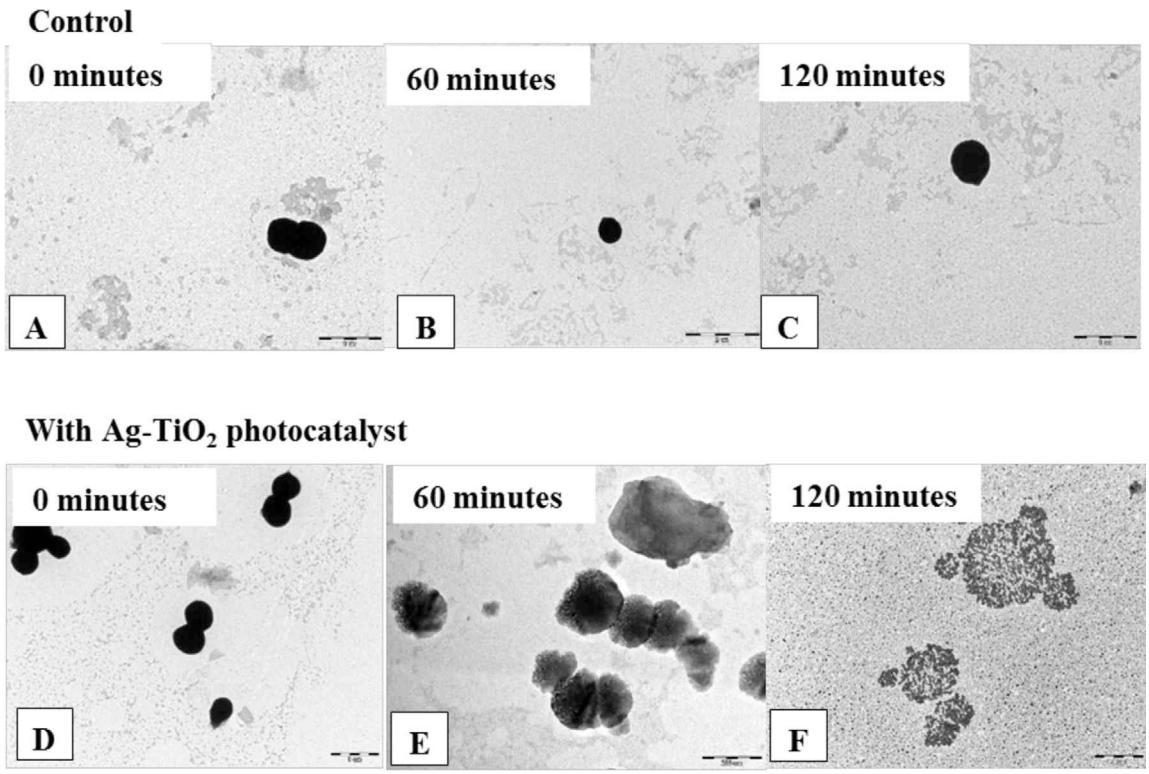

Fig. 8. Representative TEM images of the sacculi of *S. aureus*; before reaction (A) and after 60 min (B) and 120 min (C) of only visible light photocatalysis under illumination with LED-light source ($\lambda = 405$ nm) as control measurements and after 0 (D), 60 (E) and 120 min (F)) on Ag–TiO_2 photocatalyst under the same conditions.

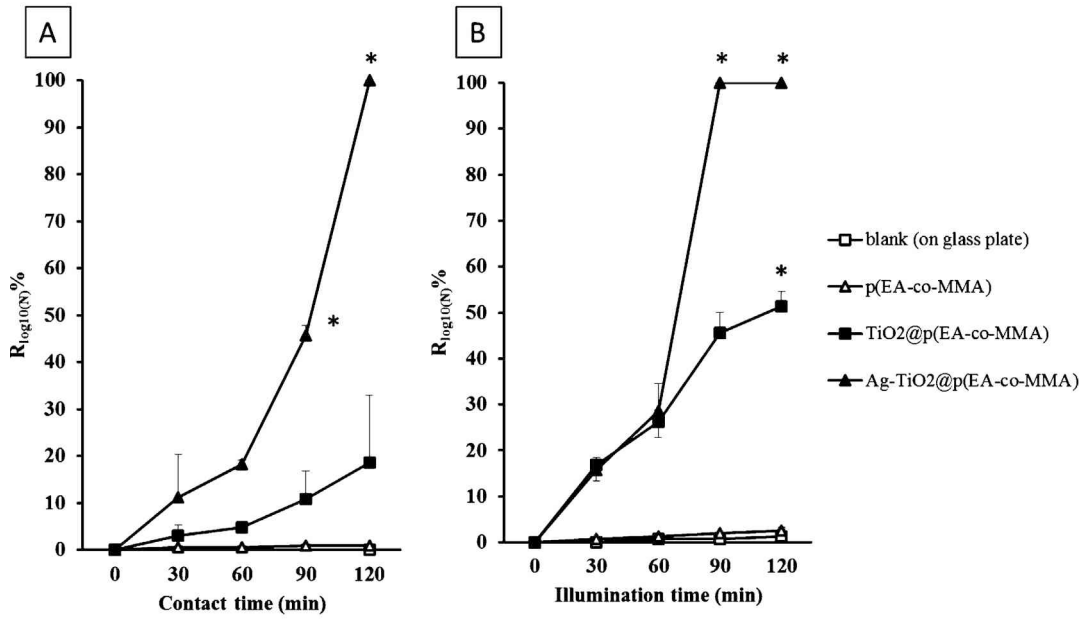

Fig. 10. The antibacterial efficiency of Ag–TiO_2/polymer films measured by modified ISO 27447:2009 standard for *P. aeruginosa* under LED-light illumination (A); and in the dark (B) with statistical analysis: $^*p < 0.05$ vs. blank.

found that the *P. aeruginosa* contains the most surface charge resulting in 2.55 g to 10^9 cfu electrostatically adhered TiO_2. Based on our experiments MRSA contains less surface charge groups on the surface (−0.89 μeq/10^9 cfu) than GR− bacteria (−1.33 μeq/10^9 cfu; −3.19 μeq/10^9 cfu) which corresponds to our surface charge experiment against TiO_2 NPs (only 0.61 g/10^9 cfu). The measured surface charge value of Ag–TiO_2 photocatalyst was lower (+0.38 meq/100 g) than the initial P25 TiO_2 (+12.3 meq/100 g) at pH 4.5 indicating the presence of Ag NPs on the surface of TiO_2. The most photocatalyst-sensitive bacteria was MRSA, despite the lowest adhesion power to surface of the photocatalyst. The results of antibacterial tests can be explained with the structure of the bacterial cell wall. The outer part of cell wall of GR+ MRSA consists only peptidoglycan, so it is much more vulnerable to external influences, as TEM pictures presents (Figs. 7 and 8). According to the above mentioned structural information it was established that 61.35% of MRSA was

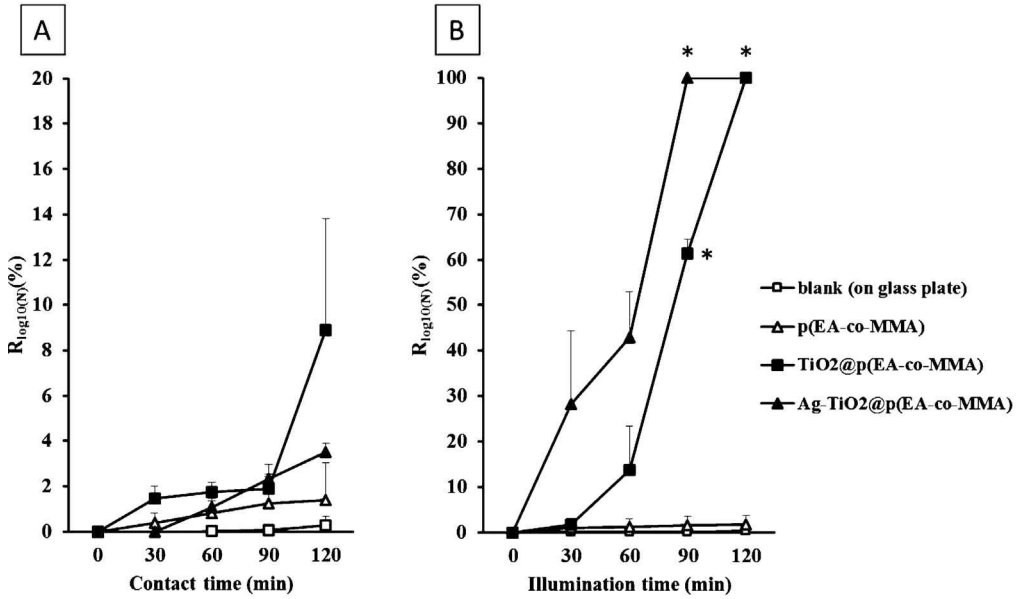

Fig. 11. The antibacterial efficiency of Ag–TiO_2/polymer films measured by modified ISO 27447:2009 standard for *E. coli* under LED-light illumination (A); and in the dark (B) with statistical analysis: $^*p < 0.05$ *vs.* blank.

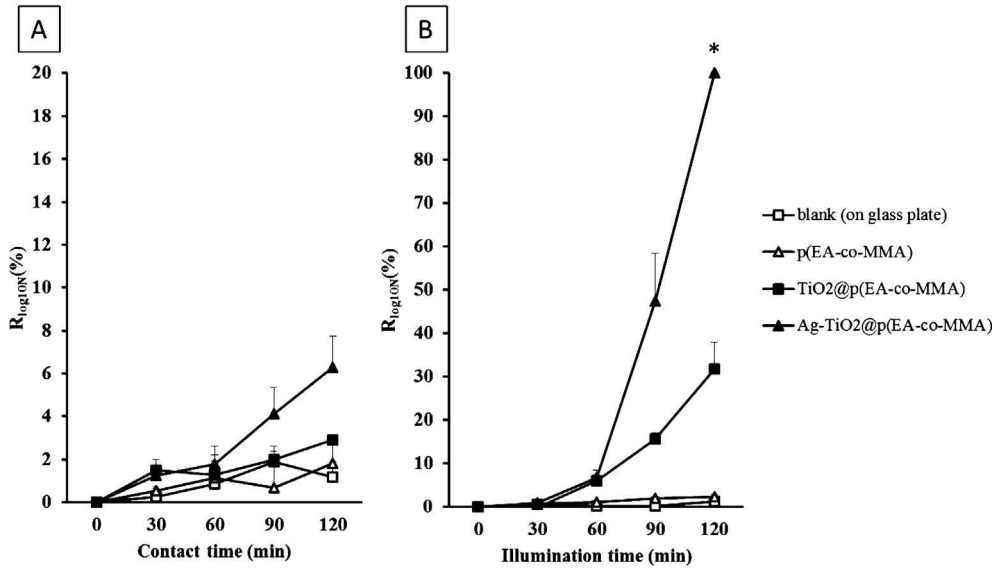

Fig. 9. The antibacterial efficiency of Ag–TiO_2/polymer films measured by modified ISO 27447:2009 standard for *S. aureus* under LED-light illumination (A); and in the dark (B) with statistical analysis: $^*p < 0.05$ *vs.* blank.

inactivated on TiO_2/polymer film after 90 min illumination while these values for GR– *P. areuginosa* and *E. coli are R*% = 45.54% and *R*% = 15.68%, respectively. Moreover, the antibacterial results are in good agreement with the adhesion measurements. Namely, the adhesion between *P. aeruginosa* and TiO_2 NPs was stronger as well as the antibacterial effect after 90 min photocatalysis. It proves, that the difference in antibacterial efficiency of photocatalysts is given with the structure of the cell wall and with the strength of bacterial adhesion power. Our optimized photoreactive nanohybrid film (0.6 mg cm^{-2} Ag–TiO_2 immobilized with 0.4 mg cm^{-2} pEA-*co*-MMA polymer) is mechanically stable, environmentally friendly and it can be activated with visible light emitting, non-harmful and power-saving LED-light sources. The developed nanohybrid films have antibacterial properties (5 log reduction of cfu in 2 h) even against antibiotic resistant bacteria (MRSA) with the ability to cause dangerous nosocomial infections. Our developed surfaces can be used in health care facilities, especially in surgery rooms as a powerful prevention against nosocomial bacteria. This application can be tested in the future on different layers (metal, special plastics, wood and wall coatings) against different multiresistant bacteria with the above-mentioned and optimized method. In this way an effective sterilizing system and prevention strategy can be developed against multiresistant human pathogen microorganisms on different surfaces.

Conflict of interest

The authors report no conflicts of interest in this work.

Acknowledgements

The authors are very thankful for the financial support from the Hungarian Scientific Research Fund (OTKA) K 116323 and K 112493

and the project named TÁMOP-4.2.6-15/1-2015-0002 and TÁMOP-4.2.1.C-14/1/KONV-2015-0013. This work was also financed by the European Union under contract no. HUSRB/1002/2.1.4/078 (DEVTEGEN) and the Hungarian National Office of Research and Technology (NKTH) under contract no. TECH-09-A2-2009-0129 (NANOSTER).

Appendix A. Supplementary data

Supplementary data associated with this article can be found, in the online version, at http://dx.doi.org/10.1016/j.apsusc.2016.02.202.

References

[1] S. Rajeshkumar, C. Malarkodi, In vitro antibacterial activity and mechanism of silver nanoparticles against foodborne pathogens, Bioinorg. Chem. Appl. (2014) 581890.
[2] P. Morganti, Use and potential of nanotechnology in cosmetic dermatology, Clin. Cosmet. Investig. Dermatol. 24 (2010) 5–13.
[3] R. Mohandas, A.A. Ejaz, Critical care: a silver lining in the quest for improved survival in sepsis, Nat. Rev. Nephrol. 10 (2014) 302–304.
[4] P.V. Gawande, A.P. Clinton, K. LoVetri, N. Yakandawala, K.P. Rumbaugh, S. Madhyastha, Antibiofilm efficacy of DispersinB(®) wound spray used in combination with a silver, Wound Dress. Microbiol. Insights 7 (2014) 9–13.
[5] A. Majdalawieh, M.C. Kanan, O. El-Kadri, S.M. Kanan, Recent advances in gold and silver nanoparticles: synthesis and applications, J. Nanosci. Nanotechnol. 14 (2014) 4757–4780.
[6] O. De Giglio, C. Coretti, G. Lovero, G. Barbuti, G. Caggiano, Pilot study on the antibacterial activity of hydrogen peroxide and silver ions in the hospital environment, Ann. Ig. 26 (2014) 181–185.
[7] A.M. Aziz, The role of healthcare strategies in controlling antibiotic resistance, Br. J. Nurs. 9 (2013) 1066–1074.
[8] R. Baxi, O.T. Mytton, M. Abid, A. Maduma-Butshe, S. Iyer, A. Ephraim, K.E. Brown, E. O'Moore, Outbreak report: nosocomial transmission of measles through an unvaccinated healthcare worker—implications for public health, J. Public Health 36 (2014) 375–381.
[9] M.K. Kaswa, M. Aloni, L. Nkuku, B. Bakoko, R. Lebeke, A. Nzita, J.J. Muyembe, B.C. de Jong, P. de Rijk, J. Verhaegen, M. Boelaert, M. Ieven, A. Van Deun, A pseudo-outbreak of pre-XDR TB in Kinshasa: a collateral damage of false fluoroquinolone resistant detection by GenoType® MTBDRsl, J. Clin. Microbiol. 52 (2014) 2876–2880.
[10] M. Dulon, C. Peters, A. Schablon, A. Nienhaus, MRSA carriage among healthcare workers in non-outbreak settings in Europe and the United States: a systematic review, BMC Infect. Dis. 14 (2014) 363.
[11] C.W. Dunnill, I.P. Parkin, Nitrogen-doped TiO_2 thin films: photocatalytic applications for healthcare environments, Dalton Trans. 40 (2011) 1635–1640.
[12] G. Fu, P.S. Vary, C.T. Lin, Anatase TiO_2 nanocomposites for antimicrobial coatings, J. Phys. Chem. B 12 (2005) 8889–8898.
[13] C.C. Peng, M.H. Yang, W.T. Chiu, C.H. Chiu, C.S. Yang, Y.W. Chen, K.C. Chen, R.Y. Peng, Composite nano-titanium oxide-chitosan artificial skin exhibits strong wound-healing effect-an approach with anti-inflammatory and bactericidal kinetics, Macromol. Biosci. 8 (2008) 316–327.
[14] L. Ye, R. Pelton, M.A. Brook, C.D. Filipe, H. Wang, L. Brovko, M. Griffiths, Targeted disinfection of *E. coli* via bioconjugation to photoreactive TiO_2, Bioconjug. Chem. 24 (3) (2013) 448–455.
[15] W.J. Chen, Y.C. Chen, Fe_3O_4/TiO_2 core/shell magnetic nanoparticle-based photokilling of pathogenic bacteria, Nanomedicine (Lond.) 5 (10) (2010) 1585–1593.
[16] M.F. Brugnera, M. Miyata, G.J. Zocolo, C.Q. Leite, M.V. Zanoni, A photoelectrocatalytic process that disinfects water contaminated with *Mycobacterium kansasii* and *Mycobacterium avium*, Water Res. 47 (2013) 6596–6605.
[17] E. Unosson, E.K. Tsekoura, H. Engqvist, K. Welch, Synergetic inactivation of *Staphylococcus epidermidis* and *Streptococcus mutansin* a TiO_2/H_2O_2/UV system, Biomatter 3 (2013) 26727.
[18] G. Rodríguez-Gattorno, P. Santiago-Jacinto, L. Rendon-Vázquez, J. Németh, I. Dékány, D. Díaz, Novel synthesis pathway of ZnO nanoparticles from the spontaneous hydrolysis of zinc carboxylate salts, J. Phys. Chem. B 107 (2003) 12597–12604.
[19] L. Kőrösi, A. Oszkó, G. Galbács, A. Richardt, V. Zöllmer, I. Dékány, Structural properties and photocatalytic behaviour of phosphate-modified nanocrystalline titania films, Appl. Catal. B: Environ. 77 (2007) 175–183.
[20] I. Dékány, L. Turi, A. Szűcs, Z. Király, Preparation of semiconductor and transition metal nanoparticles on colloidal solid supports, Colloids Surf. A: Physicochem. Eng. Aspects 3 (1998) 405–417.
[21] K. Gupta, R.P. Singh, A. Pandey, A. Pandey, Photocatalytic antibacterial performance of TiO2 and Ag-doped TiO_2 against *S aureus*, *P. aeruginosa* and *E. coli*, Beilstein J. Nanotechnol. 4 (2013) 345–351.
[22] J. Liu, Y. Ge, L. Xu, Study of antibacterial effect of polymethyl methacrylate resin base containing Ag–TiO_2 against *Streptococcus mutans* and *Saccharomyces albicans* in vitro, Hua Xi Kou Qiang Yi Xue Za Zhi 30 (2012) 201–205.
[23] G. Colon, B.C. Ward, T.J. Webster, Increased osteoblast and decreased *Staphylococcus epidermidis* functions on nanophase ZnO and TiO_2, J. Biomed. Mater. Res. A. 78 (2006) 595–604.
[24] N. Nataraj, G.S. Anjusree, A.A. Madhavan, P. Priyanka, D. Sankar, N. Nisha, S.V. Lakshmi, R. Jayakumar, A. Balakrishnan, R. Biswas, Synthesis and anti-staphylococcal activity of TiO_2 nanoparticles and nanowires in ex vivo porcine skin model, J. Biomed. Nanotechnol. 10 (2014) 864–870.
[25] Z. Bin, Z. Xu, L. Huijuan, Q. Jiuhui, C.P. Huang, Visible-light sensitive cobalt-doped $BiVO_4$ (Co–$BiVO_4$) photocatalytic composites for the degradation of methylene blue dye in dilute aqueous solutions, Appl. Catal. B: Environ. 99 (2010) 214–221.
[26] R. Nakano, H. Ishiguro, Y. Yao, J. Kajioka, A. Fujishima, K. Sunada, M. Minoshima, K. Hashimoto, Y. Kubota, Photocatalytic inactivation of influenza virus by titanium dioxide thin film, Photochem. Photobiol. Sci. 11 (2012) 1293–1298.
[27] A. Fujishima, K. Honda, Electrochemical photocatalysis of water at semiconductor electrode, Nature 238 (1972) 27–38.
[28] A. Fujishima, K. Hashimoto, T. Watanabe, TiO_2 Photocatalysis: Fundamentals and Applications, Japan.BKC Inc., 1992.
[29] L. Ge, G. Na, S. Zhang, H. Ren, Z. Yao, New insights into the aquatic photochemistry of fluoroquinolone antibiotics: direct photodegradation hydroxyl-radical oxidation, and antibacterial activity changes, Sci. Total Environ. 15 (2015) 527–528.
[30] I. Fenoglio, J. Ponti, E. Alloa, M. Ghiazza, I. Corazzari, R. Capomaccio, D. Rembges, S. Oliaro-Bosso, F. Rossi, Singlet oxygen plays a key role in the toxicity and DNA damage caused by nanometric TiO_2 in human keratinocytes, Nanoscale 21 (2013) 6567–6576.
[31] K.S. Butler, B.J. Casey, G.V. Garbocauskas, B.J. Dair, R.K. Elespuru, Assessment of titanium dioxide nanoparticle effects in bacteria: association, uptake, mutagenicity, co-mutagenicity and DNA repair inhibition, Mutat. Res. Genet. Toxicol. Environ. Mutagen. (2014), http://dx.doi.org/10.1016/j.mrgentox.2014.04.008.
[32] B. Van Aken, L.S. Lin, Effect of the disinfection agents chlorine UV irradiation, silver ions, and TiO2 nanoparticles/near-UV on DNAmolecules, Water Sci. Technol. 64 (2011) 1226–1232.
[33] G. Gogniat, S. Dukan, TiO_2 photocatalysis causes DNA damage via fenton reaction-generated hydroxyl radicals during the recovery period, Appl. Environ. Microbiol. 73 (2007) 7740–7743.
[34] B. Djordevic, W. Szybalski, Genetics of human cell lines. III. Incorporation of 5-bromo- and 5-iododeoxyuridine into the deoxyribonucleic acid of human cells and its effect on radiation sensitivity, J. Exp. Med. 112 (1960) 509–531.
[35] M. Pratap Reddy, A. Venugopal, M. Subrahmanyam, Hydroxyapatite-supported Ag–TiO_2 as *Escherichia coli* disinfection photocatalyst, Water Res. 41 (2007) 379–386.
[36] Y. Jiaguo, X. Jianfeng, C. Bei, L. Shengwei, Fabrication and characterization of Ag–TiO_2 multiphase nanocomposite thin films with enhanced photocatalytic activity, Appl. Catal. B: Environ. 60 (2005) 211–221.
[37] M.A. Arenas, C. Pérez-Jorge, A. Conde, E. Matykina, J.M. Hernández-López, R. Pérez-Tanoira, J.J. de Damborenea, E. Gómez-Barrena, J. Esteba, Doped TiO_2 anodic layers of enhanced antibacterial properties, Colloids Surf. B Biointerfaces 105 (2013) 106–112.
[38] R. Asahi, T. Morikawa, T. Ohwaki, K. Aoki, Y. Taga, Visible-light photocatalysis in nitrogen-doped titanium oxides, Science 293 (2001) 269–271.
[39] R.P. Suri, H.M. Thornton, M. Muruganandham, Disinfection of water using Pt- and Ag-doped TiO2 photocatalysts, Environ. Technol. 33 (2012) 1651–1659.
[40] N.P. Boks, W. Norde, H.C. van der Mei, H.J. Busscher, Forces involved in bacterial adhesion to hydrophilic and hydrophobic surfaces, Microbiology 154 (2008) 3122–3133.
[41] A. Terada, T. Yuasa, S. Kushimoto, A. Tsuneda, M. Katakai, M. Tamada, Bacterial adhesion to and viability on positively charged polymer surfaces, Microbiology 152 (2006) 3575–3583.
[42] F.C. Neuhaus, J. Baddiley, A continuum of anionic charge: structures and functions of D-alanyl-teichoic acids in gram-positive bacteria, Microbiol. Mol. Biol. Rev. 67 (2003) 686–723.
[43] W. Jerrold, V. Michael, E. Peter, Role of charge and hydrophobic interactions in the action of bactericidal/permeability-increasing protein of neutrophils on Gram-negative bacteria, J. Clin. Invest. 71 (1983) 540–549.
[44] Á. Veres, L. Janovák, T. Bujdosó, T. Rica, E. Fodor, Sz. Tallósy, N. Buzás, E. Nagy, I. Dékány, Silver and phosphate functionalized reactive TiO_2/polymer composite films for destructions of resistant bacteria using visible light, J. Adv. Oxid. Technol. 15 (2012) 205–216.
[45] S.P. Tallósy, L. Janovák, J. Ménesi, E. Nagy, Á. Juhász, L. Balázs, I. Deme, N. Buzás, I. Dékány, Investigation of the antibacterial effects of silver-modified TiO_2 and ZnO plasmonic photocatalysts embedded in polymer thin films, Environ. Sci. Pollut. Res. Int. 21 (2014) 11155–11167.
[46] C. Jung-Chuan, L.L. Pin, Study on pH at the point of zero charge of TiO_2 pH ion-sensitive field effect transistor made by the sputtering method, Thin Solid Films 476 (2005) 157–161.
[47] S.S. Block, in: S.S. Block (Ed.), Definition of terms in Disinfection, Sterilization and Preservation, 5th ed., Lippincott Williams & Wilkins, Philadelphia, 2001, pp. 19–28.
[48] L.F. Liu, J. Barford, K.L. Yeung, G. Si, Non-UV based germicidal activity of metal-doped TiO_2 coating on solid surfaces, J. Environ. Sci. (China) 19 (2007) 745–750.

[49] C. Laflamme, S. Lavigne, J. Ho, C. Duchaine, Assessment of bacterial endospore viability with fluorescent dyes, J. Appl. Microbiol. 96 (2004) 684–692.
[50] B. Glauner, Separation and quantification of muropeptides with high-performance liquid chromatography, Anal. Biochem. 172 (1988) 451–464.
[51] J. Krýsa, E. Musilová, J. Zita, Critical assessment of suitable methods used for determination of antibacterial properties at photocatalytic surfaces, J. Hazard Mater. 195 (2011) 100–106.
[52] Z. Xiaoshan, C. Yung, C. Yongsheng, Toxicity and bioaccumulation of TiO_2 nanoparticle aggregates in *Daphnia magna*, Chemosphere 78 (2010) 209–215.
[53] T. Sawada, F. Yoshino, K. Kimoto, Y. Takahashi, T. Shibata, N. Hamada, T. Sawada, M. Toyoda, Coated with fluoridated apatite ESR detection of ROS generated by TiO2, J. Dent. Res. 89 (2010) 848–853.
[54] J.F. Perez-Benito, Iron(III)-hydrogen peroxide reaction: kinetic evidence of a hydroxyl-mediated chain mechanism, J Phys. Chem. A 108 (2004) 4853–4858.
[55] T. Preocanin, N. Kállay, Point of zero charge and surface charge density of TiO_2 in aqueous electrolyte solution as obtained by potentiometric mass titration, Croat. Chem. Acta 79 (2006) 95–106.
[56] S.M. Stocks, Mechanism and use of the commercially available viability stain, BacLight, Cytometry Part A 61 (2004) 189–195.
[57] W.E. Goldstein, in: W.E. Goldstein (Ed.), Pharmaceutical Accumulation in the Environment: Prevention, Control, Health Effects, and Economic Impact, CRC Press, Boca Raton, FL, 2014, pp 262.
[58] UPAC-IUB Joint Commission on Biochemical Nomenclature (JCBN), Nomenclature of glycoproteins, glycopeptides and peptidoglycans, Eur. J. Biochem. 159 (1986) 1–6.
[59] J. van Heijenoort, Formation of the glycan chains in the synthesis of bacterial peptidoglycan, Glycobiology 11 (2001) 25–36.
[60] A.J. Kora, J. Arunachalam, Assessment of antibacterial activity of silver nanoparticles on *Pseudomonas aeruginosa* and its mechanism of action, World J. Microbiol. Biotechnol. 27 (2010) 1209–1216.
[61] G. Zhao, S.E. Stevens, Multiple parameters for the comprehensive evaluation of the susceptibility of *Escherichia coli* to the silver ion, Biometals 11 (1998) 27.
[62] W.J. Schreurs, H. Rosenberg, Effect of silver ions on transport and retention of phosphate by *Escherichia coli*, J. Bacteriol. 152 (1982) 7–13.